amino acids that participate in cytokinesis. A random fragment library of Mid1 cDNA was generated using tagged random primer PCR (tPCR). The fragment library was cloned upstream of a monomeric enhanced GFP (mEGFP) and expressed in *E.coli*. The GFP fluorescence of the bacterial colonies expressing the fusion constructs were compared to a threshold level of fluorescence to test if the Mid1 fragment fused to mEGFP is folded. Colonies expressing folded fragments of Mid1 are brighter than control colonies or colonies expressing an unfolded protein fragment fused upstream of mEGFP. Approximately 27000 colonies were screened to identify five soluble folded domains and one insoluble region, accounting for the entire length of Mid1 protein. This large scale approach will be useful in rapidly mapping domain boundaries of proteins in absence of any prior knowledge about the domain organization of the proteins.

34-Plat
A Protein Interaction Network generated from Streptococcus Pneumoniae
Doron Gerber, Sebastian J. Maerkl, Stephen R. Quake.
Stanford University, Stanford, CA, USA.
Mapping protein interaction network topologies represents a fundamental step towards a proteome-wide understanding of biological processes. The current high-throughput methods used for protein interactions are yeast two hybrid and affinity purification coupled with mass spectrometry, but both systems require cumbersome cloning steps, are challenging to automate, and have limited ability to detect weak or transient interactions. To overcome these disadvantages we developed a microfluidic in vitro protein expression and interaction platform based on a highly parallel and sensitive microfluidic affinity assay. We used this system to perform 14,792 on-chip experiments which exhaustively measure the protein-protein interaction network of 43 Streptococcus pneumoniae proteins. The resulting network of 157 interactions is denser than one would expect based on the existing data from E. coli and H. pylori. The network shows evidence of being scale free, with the most highly connected nodes derived from chaperones. Analysis of the network reveals previously undescribed physical interactions members of some biochemical pathways.

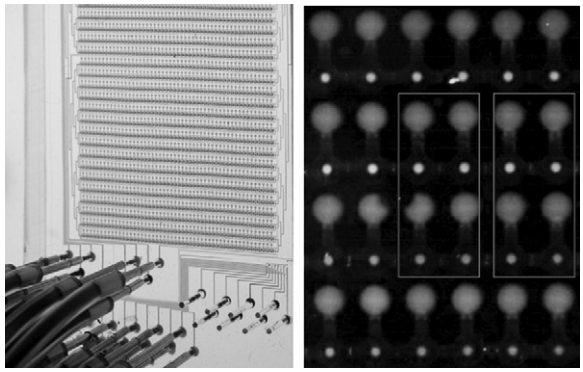

Left panel - Microfluidic device loaded with food-dyes. Flow lines (blue), ''Sandwich, Neck valves and Button valves'' (red, yellow and green) used for performing PING. Right panel - example of 2 protein-protein interactions (orange).

35-Plat
Diversity-Based Design of Synthetic Gene Networks with Desired Functions
Xiao Wang, Tom Ellis, James J. Collins.
Boston University, Boston, MA, USA.
Constructing predictable gene networks with desired functions remains hampered by the lack of well-characterized components and the fact that assembled networks often require extensive, iterative retrofitting for optimization. Here we present an approach where network components are synthesized with random sequences incorporated into their design, giving rapid parallel production of component libraries with inherent diversity. When coupled with in silico modeling, libraries present a choice of characterized parts for gene network design, and those optimal for the desired function can be selected for network assembly, without the need for post-hoc tweaking. We validated our approach in yeast (S.cerevisiae) by synthesizing a regulatory promoter library and using it to construct negative feedforward loop networks with different, desired input-output characteristics. We then implemented the method to produce a synthetic gene network that acts as a timer, tunable by component choice. We utilize this network to control the timing of the yeast flocculation phenotype, which is crucial to brewing, illustrating a practical application of our approach.

Platform C: Oxidative Phosphorylation & Mitochondrial Metabolism

36-Plat
Molecular Basis of Substrate Selectivity in the ADP/ATP Carrier
Yi Wang, Emad Tajkhorshid.
University of Illinois at Urbana-Champaign, Urbana, IL, USA.
The ADP/ATP carrier (AAC) is a membrane transporter that mediates the exchange of ADP and ATP across the mitochondrial inner membrane. During an exchange cycle, AAC switches between two conformational states, the cytoplasm-open state (c-state), and the matrix-open state (m-state). Our recent molecular dynamics simulations revealed spontaneous binding of ADP to the c-state AAC, and identified the unknown binding site for ADP as a pocket deeply positioned inside the lumen that forms through significant conformational changes of several basic residues in response to substrate binding. We also showed that ADP binding likely triggers AAC transition to the m-state by breaking a salt bridge network. The identified binding site has allowed us to explore substrate selectivity in AAC by simulating the ''binding'' of various ligands, e.g., AMP and Mg-ADP, to AAC. AMP does bind but is not transported by AAC, and Mg is known to have an inhibitory effect on AAC. However, the molecular details involved in these processes are largely unknown. Our results suggest that the presence of a minimum of two phosphate groups in their Mg-free form is absolutely necessary for proper binding and for initiating the structural changes required for activation of AAC. AMP and Mg-ADP cannot establish sufficient contact with the salt bridge ring at the bottom of AAC lumen, either due to lack of the beta-phosphate in AMP, or interference of $Mg2+$ with the phosphate groups in Mg-ADP. These results provide additional evidence for the ADP binding site characterized in our earlier study, and suggest a mechanism for substrate selectivity in AAC.

37-Plat
VDAC Regulation by Cytosolic Proteins
Tatiana K. Rostovtseva.
NICHD, NIH, Bethesda, MD, USA.
Voltage-dependent anion channel VDAC, positioned on the interface between mitochondria and the cytosol, is at the control point of mitochondria life and death. This large channel plays the role of a ''switch'' that defines in which direction mitochondria will go: to normal respiration or to suppression of mitochondria metabolism that leads to apoptosis and cell death. As the most abundant protein in the mitochondrial outer membrane (MOM), VDAC is known to be responsible for ATP/ADP exchange and for the fluxes of other metabolites across MOM. It controls them by switching between the open and ''closed'' states that are virtually impermeable to ATP and ADP. This control has dual importance: in maintaining normal mitochondria respiration and in triggering apoptosis when cytochrome c and other apoptogenic factors are released from the intermembrane space into the cytosol. Emerging evidence indicates that VDAC closure promotes apoptotic signals without direct involvement of VDAC in the permeability transition pore or hypothetical Bax-containing cytochrome c permeable pores. Closure of VDAC induced by such dissimilar cytosolic proteins as pro-apoptotic tBid and dimeric tubulin is compared to show that the involved mechanisms are rather distinct. While tBid mostly modulates VDAC voltage gating, tubulin blocks the channel with the efficiency of blockage controlled by voltage. Tubulin strikingly increases voltage sensitivity of VDAC reconstituted into planar phospholipid membrane and could induce VDAC closure at < 10 mV transmembrane potentials. Experiments with isolated mitochondria confirm a tubulin-induced VDAC closure. Our findings suggest a novel mechanism of regulation of mitochondrial energetics, governed by VDAC and tubulin at the mitochondria-cytosol interface. Overall, we demonstrate that VDAC gating is not just an observation made under artificial conditions of channel reconstitution but is a major mechanism of MOM permeability control.

38-Plat
A Microcompartment Of Mitochondrial Nucleoside Diphosphate Kinase: Cardiolipin Interaction And Coupling Of Nucleotide Transfer With Respiration
Uwe Schlattner[1], Malgorzata Tokarska-Schlattner[1], Ivan Dinh[1], Mathieu Boissan[2], Marie-Lise Lacombe[2].
[1]Inserm, U884, Univ Joseph Fourier, Grenoble 1, Grenoble, France, [2]Inserm, UMR S893, CdR Saint-Antoine, UMPC Univ Paris 6, Paris, France.
Molecular functions of mitochondrial nucleoside diphosphate kinase (NDPK-D) were studied using different biophysical and biochemical techniques. Subfractionation of rat liver and HEK 293 cell mitochondria revealed that NDPK-D is essentially bound to the inner membrane. The kinase interacted electrostatically with anionic phospholipids, showing highest affinity for cardiolipin as

quantified by surface plasmon resonance. NDPK-D was also able to cross-link anionic phospholipid-containing liposomes as seen in light scattering assays, suggesting that the hexameric kinase could promote intermembrane contacts. Mutation of the central arginine (R90) in a surface exposed basic RRK motif unique to NDPK-D strongly reduced these membrane interactions. In a model using HeLa cells naturally almost devoid of NDPK-D, wt protein and R90D mutant were stably expressed, but only wt protein was found attached to membranes. Respiration was significantly stimulated by the NDPK substrate TDP only in mitochondria containing wt NDPK-D, but not in those expressing R90D mutant that is catalytically equally active. This indicates local ADP regeneration in the mitochondrial intermembrane space and a tight functional coupling of NDPK-D with oxidative phosphorylation that depends on the membrane-bound state of the kinase. A model is proposed for a mitochondrial NDPK microcompartment.

39-Plat

Using Two-photon Excited Fluorescence Intensity- and Lifetime-based NADH Imaging to Investigate Cochlea Metabolism

LeAnn M. Tiede, Jorge A. Vergen, Clifford Hecht, Richard Hallworth, Michael G. Nichols.
Creighton University, Omaha, NE, USA.

Metabolism and mitochondrial dysfunction are thought to be involved in many different hearing disorders including noise induced hearing loss and presbycusis. We have employed two-photon fluorescence imaging of intrinsic mitochondrial reduced nicotinamide adenine dinucleotide (NADH) to study the metabolic status of the different cell types in excised yet intact mouse organ of Corti preparations. Recent published studies employ fluorescence lifetime imaging (FLIM) to determine the ratio of the free to enzyme-bound fluorophores populations that occur during changes in metabolism. We have compared traditional intensity based methods to FLIM in order to evaluate the two different methods in both cultured cells and the excised organ of Corti. Treatment with both metabolic uncouplers and inhibitors caused systematic shifts in both the lifetime and populations of the free and bound pools of NADH, resulting in significant differences in the calculated concentration of NADH when compared to using intensity alone to calculate the same value. Mapping of the locations of the individual lifetimes, shows that the lifetime of NADH varies in different cellular locations as well as in different cell types. Possible implications for the study of hearing loss will be discussed.

Supported by NIH DC 08895, NIH P20 RR016475 from the INBRE Program of the National Center for Research Resources., and NIH R15-GM085776.

40-Plat

Mitochondrial Energy Metabolism and Ca^{2+} Handling in Pancreatic Beta-cells. A System Analysis Approach

Leonid E. Fridlyand, Louis H. Philipson.
University of Chicago, Chicago, IL, USA.

Pancreatic islet beta-cells respond to rising blood glucose by increasing oxidative metabolism, leading to both an increased mitochondrial membrane potential (Ψm) and ATP/ADP ratio in cytoplasm. This leads to a closure of K_{ATP} channels, depolarization of the plasma membrane, influx of calcium and the eventual secretion of insulin. Such a signaling mechanism suggests that mitochondrial metabolism and ATP/ADP ratio regulation in beta-cells may be specially coupled in comparison with other cell types. We performed mathematical modeling to quantitatively assess how cytoplasmic ATP/ADP ratio can be controlled by mitochondria. The cytoplasmic part of the model includes glucokinase, glycolysis, pyruvate reduction, NADH and ATP production and consumption. The mitochondrial part of the model includes production of NADH, which is regulated by pyruvate dehydrogenase. NADH is used in the electron transport chain to establish a proton motive force, driving the F_1F_0-ATPase. Mitochondrial matrix Ca^{2+} is determined by the Ca^{2+} uniporter and Na^+/Ca^{2+} exchanger. The model is described by ordinary differential equations for cytoplasmic and mitochondrial parameters. The model simulates the response of the ATP/ADP ratio to changes in substrate delivery, to inhibition of the mitochondrial Ca^{2+} exchanger and other effects. We found that mitochondrial Ψm should be in a range lower than 150 mV (where F_1F_0-ATPase is sensitive to Ψm) to provide a sensitivity of the ATP/ADP ratio to glucose in beta-cells. On other hand, Ψm can work in the range above 150 mV to provide a maximal F_1F_0-ATPase productivity in other cell types (for example in myocytes). Kinetic analysis of the model reveals that these differences can be simulated by a decreased respiratory activity and higher leak capacity in beta-cell mitochondria in comparison with muscle cell mitochondria that were found recently by Affourtit and Brand (2006).

41-Plat

Modeling Regulation of Mitochondrial Free Ca^{2+} by ATP/ADP-Dependent Ca^{2+} Buffering

Ranjan K. Dash, Matthew D. Thompson, Kalyan C. Vinnakota, Johan Haumann, Mohammed Aldakkak, Amadou K.S. Camara, David F. Stowe, Beard A. Daniel.
Medical College of Wisconson, Milwaukee, WI, USA.

Introduction: Mitochondrial free $[Ca^{2+}]$ ($[Ca^{2+}]_m$) is regulated by cation fluxes through the Ca^{2+} uniporter (CU), Na^+/Ca^{2+} exchanger (NCE), Na^+/H^+ exchanger (NHE), and Ca^{2+}/H^+ exchanger (CHE) as well as via Ca^{2+} buffering by the mitochondrial proteins. However, the regulation of $[Ca^{2+}]_m$ via ATP/ADP-dependent dynamic Ca^{2+} buffering mechanism inside the mitochondrial matrix during transient state-3 respiration is not well known. **Methods:** To gain a quantitative understanding of this Ca^{2+} buffering phenomenon, we developed a computational model of mitochondrial bioenergetics and Ca^{2+} handling by integrating our recent biophysical models of the CU, NCE, NHE, and CHE into our well-validated model of mitochondrial oxidative phosphorylation, TCA cycle, and electrophysiology. The model also accounts for binding and buffering of cations with metabolites, including ATP, ADP and Pi. Experiments were performed to spectrofluorometrically measure $[Ca^{2+}]_m$, pH_m, membrane potential ($\Delta\Psi_m$), and NADH redox state in guinea pig heart mitochondria suspended in Na^+ and Ca^{2+} free buffer medium (ensured with ~50 μM of EGTA) with 0.5 mM pyruvic acid (HPyr). Dynamics were inferred with various addition of $CaCl_2$ (0, 10, 25 μM of $CaCl_2$; 16, 88, 130 nM of free $[Ca^{2+}]$ followed by 250 μM of ADP in the presence or absence of carboxyatractyloside (ANT blocker) and oligomycin (F_1F_0-ATPase blocker). **Results and Discussion:** Model analysis of the data on (i) initial decrease of $[Ca^{2+}]_m$ with addition of Na^+-independent substrate HPyr, and (ii) transient increases of $[Ca^{2+}]_m$ with addition of ADP suggests ATP/ADP-dependent dynamic Ca^{2+} buffering inside the cardiac mitochondrial matrix. This model will be helpful to understand mechanisms by which $[Ca^{2+}]_m$ both regulates, and is modulated by, mitochondrial energy metabolism.

42-Plat

The External Stalk of the FoF1-ATPase: 3D-Structure of the b-Dimer

Oleg A. Volkov, Susan J. Pandey, John G. Wise, **Pia D. Vogel**.
Southern Methodist University, Dallas, TX, USA.

The structure of the external stalk of the FoF1-ATP synthase and its function during catalysis remain one of the important questions in bioenergetics.

Proteomics, structure prediction, molecular modeling and ESR spectroscopy using site-directed spin labeling were employed to elucidate the structure and interfacial packing of the E. coli b-subunit homodimeric and Synechocystis bb' heterodimeric stalks of ATP synthases.

b-Subunits of different origin demonstrate little sequence similarity. Structure prediction algorithms, however, showed that all of the compared sequences contain extensive heptad repeats, suggesting that these proteins may favorably pack as left-handed coiled coils (LHCC).

Molecular modeling of homo- and heterodimeric b produced low energy LHCC. Extensive mutagenesis followed by site-directed spin labeling and subsequent ESR investigations in soluble homo- and heterodimeric b-constructs allowed the determination of inter- and intra-subunit distances.

Inter-spin distances obtained by ESR agreed very well with distances derived from LHCC molecular models of b- and bb'-dimers and therefore strongly support our proposition that dimeric external stalks of ATP synthases indeed form left-handed coiled coils.

The extreme C-terminal part of the b-dimer is not predicted to form a coiled coil structure. We are presently investigating this part of the second stalk both when in solution and when in complex with soluble F1-ATPase. The influence of subunit δ is of particular interest due to its proposed direct interaction with the C-terminus of subunit b.

Initial site-directed spin labeling and ESR experiments using complete E. coli FoF1-ATP synthase indicate that the inter-subunit packing of the b-dimer changes during catalytic turnover, which may be a mechanism for elastic coupling of the different rotating parts of the enzyme.

43-Plat

Torque Generation Mechanism of ATP Synthase and Other Rotary Motors

John H. Miller[1], Vijayanand Vajrala[1], Hans L. Infante[1], James R. Claycomb[2].
[1]University of Houston, Houston, TX, USA, [2]Houston Baptist University, Houston, TX, USA.

Ion driven rotary motors, including F0-ATP synthase (F0) and the bacterial flagellar motor, convert energy from ion translocation into torque and rotary